PPAR-gamma pathways attenuate pulmonary granuloma formation in a carbon nanotube induced murine model of sarcoidosis

Matthew McPeek[a], Anagha Malur[a], Debra A. Tokarz[b], Gina Murray[c], Barbara P. Barna[a], and Mary Jane Thomassen[a,*]

[a]Department of Internal Medicine, Pulmonary, Critical Care & Sleep Medicine, Brody School of Medicine, East Carolina University, Greenville, NC, 27834, USA

[b]Department of Population Health and Pathobiology, College of Veterinary Medicine, North Carolina State University, Raleigh, NC, 27695, USA

[c]Department of Pathology, Brody School of Medicine, East Carolina University, Greenville, NC, 27834, USA

Abstract

Peroxisome proliferator activated receptor gamma (PPARγ), a ligand activated nuclear transcription factor, is constitutively expressed in alveolar macrophages of healthy individuals. PPARγ deficiencies have been noted in several lung diseases including the alveolar macrophages of pulmonary sarcoidosis patients. We have previously described a murine model of multiwall carbon nanotubes (MWCNT) induced pulmonary granulomatous inflammation which bears striking similarities to pulmonary sarcoidosis, including the deficiency of alveolar macrophage PPARγ. Further studies demonstrate alveolar macrophage PPARγ deficiency exacerbates MWCNT-induced pulmonary granulomas. Based on these observations we hypothesized that activation of PPARγ via administration of the PPARγ-specific ligand rosiglitazone would limit MWCNT-induced granuloma formation and promote PPARγ-dependent pathways. Results presented here show that rosiglitazone significantly limits the frequency and severity of MWCNT-induced pulmonary granulomas. Furthermore, rosiglitazone attenuates alveolar macrophage NF-κB activity and downregulates the expression of the pro-inflammatory mediators, CCL2 and osteopontin. PPARγ activation via rosiglitazone also prevents the MWCNT-induced deficiency of PPARγ-regulated ATP-binding cassette lipid transporter-Gl (ABCG1) expression. ABCG1 is crucial to pulmonary lipid homeostasis. ABCG1 deficiency results in lipid accumulation which promotes pro-inflammatory macrophage activation. Our results indicate that restoration of homeostatic ABCG1 levels by rosiglitazone correlates with both reduced pulmonary lipid accumulation, and decreased alveolar macrophage activation. These data confirm and further support our previous observations that PPARγ pathways are critical in regulating MWCNT-induced pulmonary granulomatous inflammation.

[*]Corresponding author. Brody School of Medicine, East Carolina University, 600, Moye Blvd/3E-149, Greenville, NC, 27834, USA., *address*: thomassenm@ecu.edu (M.J. Thomassen).

Keywords

1. Introduction

Granulomatous lung diseases represent a significant health burden worldwide. Sarcoidosis is an inflammatory condition characterized by the presence of non-necrotizing granulomas which effects the lungs and mediastinal lymph nodes in 90% of clinical cases [1]. The etiology of sarcoidosis has not been determined, however current understanding suggest the presence of a poorly soluble antigen leading to an exuberant host immune response in genetically susceptible individuals [2]. Epidemiological studies have found a correlation between pulmonary sarcoidosis and exposure to wood-burning stoves, fireplaces and certain occupations such as firefighters [3–5]. An increased incidence of sarcoid-like granulomatous lesions have also been reported in first responders present at the September 2001 World Trade Center Disaster [6]. These environments have been shown to contain particulate matter of respirable sizes, including carbon nanotubes. Carbon nanotubes (CNT) are produced as byproducts of combustion or manufactured for a variety of commercial applications. Evaluation of the respiratory toxicology of these materials has found the potential to induce pulmonary granulomatous lesions in exposed animals [7,8]. These observations prompted our laboratory to investigate the use of multiwall carbon nanotubes (MWCNT) to generate a murine model of pulmonary granulomatous inflammation to study pulmonary sarcoidosis [9].

Previous methods utilized to induce pulmonary granulomas included the administration of pathogens or introduction of antigen bound sepharose beads into the tail vein of sensitized animals [10–12]. While these models have advanced our understanding of pulmonary granuloma formation they have notable drawbacks including the presence of active pathogens, eliciting granuloma in the pulmonary capillaries instead of the airways and a relatively short resolution time. In our studies, evaluation of mice 60 days following MWCNT instillation found the persistence of granulomatous lesions throughout the lung [9]. Further studies demonstrated that the MWCNT model closely mimics sarcoidosis pathophysiology, including elevated expression of inflammatory mediators and reduced expression and activity of alveolar macrophage peroxisome proliferator-activated receptor gamma (PPARγ) [9,13,14].

PPARγ, a ligand-activated nuclear transcription factor, has been shown to limit pro-inflammatory macrophage activation [15]. PPARγ regulates gene expression by selectively binding PPARγ-response elements, promoting target gene expression, or through the inhibition of other transcription factors such as nuclear factor- κB (NF-κB) [16,17]. PPARγ, constitutively active in alveolar macrophages of healthy individuals, is deficient in multiple lung diseases including alveolar macrophages of pulmonary sarcoidosis patients [18–20]. The importance of alveolar macrophage PPARγ to pulmonary homeostasis is demonstrated

by macrophage-specific PPARγ knockout mice. These animals exhibit increased Th-1 pro-inflammatory cytokine expression and dysregulated pulmonary lipid catabolism [21,22].

PPARγ maintains pulmonary lipid homeostasis through the expression of alveolar macrophage ATP-binding cassette lipid transporter-G1 (ABCG1) [22,23]. Following uptake by scavenger receptors, such as the PPARγ-regulated cluster of differentiation-36 (CD36), lipids are catabolized and effluxed to extracellular acceptors by ABCG1, and the complimentary lipid transporter ABCA1 [24]. Deficiency of ABCG1 or ABCA1 results in pulmonary lipid accumulation and elevated inflammatory mediators [25–28]. The inability to properly efflux cholesterol leads to increased sensitivity to extracellular inflammatory signaling in ABCA1/ABCG1 deficient macrophages [29]. Our recent studies in alveolar macrophages from sarcoidosis patients and MWCNT-instilled mice observed decreased expression of both ABCG1 and ABCA1 [30]. The deficiency of these lipid transporters correlates with increased alveolar macrophage lipid accumulation in MWCNT-instilled animals [30]. These observations suggest that downregulation of ABCG1 and ABCA1 may contribute to MWCNT-induced inflammation. We hypothesized that increase of the PPARγ-ABCG1 pathway would limit alveolar macrophage activation and pulmonary granuloma formation. To address this hypothesis we utilized the PPARγ-specific agonist rosiglitazone to activate PPARγ pathways. Results shown here indicate that rosiglitazone attenuates MWCNT-induced granulomatous inflammation.

2.   Materials and methods

2.1.   Animal care and treatment

Animal studies were conducted in accordance with the National Institutes of Health guide for the care and use of Laboratory animals and with approval from the East Carolina University Institutional Animal Care and Use Committee. C57BL/6J wild type mice were purchased from The Jackson Laboratory (Bar Harbor, ME). An equal number of age and sex matched controls were randomly assigned into experimental groups. Rosiglitazone laden diets were produced by Teklad Diets (Madison, MI), incorporating rosiglitazone (Cayman Chemical. Ann Arbor, MI) into standard rodent chow (Prolab RMH 300, LabDiet; St. Louis, MO), delivering 2, 6 or 12 mg/kg/day (TD.160572, TD.160573 and TD.160574 respectively). Diets were administered daily, three days prior to instillation of multiwall carbon nanotubes (MWCNT) until necropsy at the indicated time point.

2.2.   MWCNT model

Pulmonary granulomas were generated by oropharyngeal aspiration of 100 μg MWCNT (Cat.900–1501, Lot: GS1801) purchased from SES Research, Houston Texas as previously described [9]. Animals were euthanized with tribromoethanol and bron-choalveolar lavage (BAL) was performed for the collection of BAL cells as previously described [21]. Differential counts were performed on cytospins stained with modified Wright's stain. Histological analysis was performed on un-lavaged lungs inflated with formalin as previously described [9].

2.3. RNA purification and analysis

Total RNA was collected from BAL cell pellets with the miRNeasy Micro Kit and protocol (Qiagen. Valencia, CA). Primers were obtained from Qiagen for ATP binding cassette (ABC) transporter-A1 (Abca1, PPM03952F), Abcg1 (PPM03895A), chemokine (C-C motif) ligand-2 (Ccl2, PPM03151G), Glyceraldehyde-3-phosphate-dehy-drogenase (Gapdh, PPM02946E), peroxisome proliferator activated receptor-gamma (PPARγ, PPM05108B) and osteopontin (Spp1, PPM03648C). Relative gene expression of complimentary DNA synthesized with the RT2 First Strand Kit was evaluated on an ABI Prism 7300 system (Applied Biosystems. Foster City, CA) in comparison to Gapdh using the $2^{- \quad CT}$ method [31].

2.4. Immunohistochemistry

BAL cytospins of freshly isolated BAL cells were fixed with 4% paraformaldehyde, permeabilized with 0.3% Triton-X-100 and stained for NF-κB 1:200 (catalog# 6956 S. Cell Signaling. Danvers, MA) overnight at 4 °C followed by Alexa-conjugated goat anti mouse IgG 1:1000 (Invitrogen. Carlsbad, CA). Slides were counterstained with propidium iodide (Vector Laboratories. Burlingame, CA) to facilitate nuclear localization. Images were acquired on a LSM 700 confocal microscope (Zeiss. Oberkochen, Germany). Quantification of NF-κB nuclear localization was quantified using ZEN Blue software (Zeiss). Differential analysis of BAL cells revealed that alveolar macrophages constituted the majority of cells (93.4%– 99.7%; n 6) at either 10 or 20 days post treatment with no significant differences among BAL samples from control or treated groups.

2.5. Analysis of bronchoalveolar lavage fluid

Total cholesterol was measured using the Amplex Red Cholesterol Assay kit (Thermo Fisher Scientific. Waltham, MA) according to manufacturer's instructions in the presence of cholesterol esterase. Cholesterol was normalized to protein content of BAL Fluid measured by BCA assay (Thermo Fisher Scientific).

2.6. Quantitative analysis of tissue

Digital images of whole lung cross sections stained with hematoxylin & eosin were acquired on an Aperio ScanScope (Aperio Technologies, Inc. Vista, CA). Analysis was performed blindly on randomized digital images, scanning the entire lung at 20× magnification for pulmonary granulomas. A granuloma was defined as a carbon aggregate completely surrounded by tissue and associated with three or more cell nuclei. Quantification of total stained lung area and carbon content were performed by the Translational Pathology Lab (University of North Carolina, Chapel Hill) using the Aperio deconvolution method as previously described [32]. The length (L) and width (W) of the tracheobronchal lymph node, identified based on Van den Broeck et al. [33], was used to determine lymph node volume using the formula $(LxW^2)\pi/6$.

2.7. Statistical analysis

All data represent the mean of at least three individual experiments ±SEM unless otherwise indicated. Statistical analysis was performed using GraphPad Prizm software (San Diego,

CA). Twotailed student's t-tests were utilized for the comparison between groups. For all tests, $p < 0.05$ was considered statistically significant.

3. Results

3.1. PPARγ agonist regulates alveolar macrophage gene expression 10 days post MWCNT-Instillation

Our previous studies have shown deficiency of PPARγ, ABCA1 and ABCG1 in alveolar macrophages from both sarcoidosis patients and the 60 day MWCNT model [13,19,30]. The inflammatory mediators, chemokine (C-C motif) ligand-2 (CCL2) and osteopontin, were elevated in sarcoidosis granulomatous tissue and in the 60 day MWCNT model [13,34–36]. In the present study we evaluated gene expression of alveolar macrophages isolated 10 days following MWCNT instillation. PPARγ, ABCA1 and ABCG1 expression were significantly decreased in MWCNT-instilled animals compared to those receiving vehicle (Fig. 1A). As expected, the expression of CCL2 and osteopontin was upregulated in MWCNT-instilled mice (Fig. 1B). To determine the optimal dose of rosiglitazone required to increase alveolar macrophage ABCG1 expression and decrease the expression of pro-inflammatory mediators, rosiglitazone was administered at 2, 6 or 12 mg/kg/day. The expression of alveolar macrophage ABCG1 was significantly increased in animals receiving 6 and 12 mg/kg diet (Fig. 1C). Evaluation of pro-inflammatory mediators found rosiglitazone capable of limiting CCL2 and osteopontin expression in a dose-dependent manner (Fig. 1D and E). The optimal dose of rosiglitazone required to increase alveolar macrophage ABCG1 and limit pro-inflammatory mediator expression was 6 mg/kg (Fig. 1).

Histological examination of lung morphology confirmed our previous observation that granulomas at 10 days post-instillation were loosely formed [9]. Evaluation of the frequency and severity of granulomatous inflammation using a previously described scoring system [13], found no difference between MWCNT-instilled animals given rosiglitazone and normal chow (data not shown). To determine if the continuation of rosiglitazone would limit pulmonary granuloma formation, animals were evaluated 20 days post MWCNT instillation.

3.2. Rosiglitazone inhibits MWCNT-induced pulmonary granuloma formation

Quantitative measurements were performed on digital images of lung tissue from MWCNT-instilled mice receiving normal chow or the optimal dose of rosiglitazone (6 mg/kg). The administration of rosiglitazone 20 days post-instillation: 1) significantly decreased the number of granulomas per lung area (Fig. 2A); 2) limited the size of granulomatous lesions (Fig. 2B); and 3) reduced the total carbon deposition in the lungs compared to animals receiving normal chow (Fig. 2C). During gross dissection of the thoracic cavity, carbon deposition was noted in the cranial mediastinal lymph node. Quantification of lymph node volume revealed a significant increase following MWCNT instillation compared to mice receiving vehicle, and further lymphadenopathy in animals receiving rosiglitazone (Fig. 2D). As a measure of total lung injury, protein concentration of the BAL fluid (BALF) was evaluated. MWCNT instillation resulted in significantly higher BALF protein concentration compared to animals receiving vehicle, while administration of rosiglitazone attenuated this increase (Fig. 2E).

3.3. Rosiglitazone limits alveolar macrophage activation and pulmonary dyslipidemia following MWCNT instillation

Administration of rosiglitazone (6 mg/kg) significantly attenuated the expression of alveolar macrophage CCL2 and osteopontin expression 20 days post MWCNT instillation (Fig. 3A and B). We performed further studies to determine the mechanism by which rosiglitazone limited pro-inflammatory gene expression. PPARγ is capable of limiting pro-inflammatory gene expression through trans-repression of NF-κB activity [16,17]. Analysis of alveolar macrophages from MWCNT-instilled mice demonstrated significantly less nuclear p65 localization in animals receiving rosiglitazone laden diet compared to controls (Fig. 3C).

Decreased expression of alveolar macrophage PPARγ, ABCA1 and ABCG1 was also observed 20 days post MWCNT instillation (Fig. 4A–C). Rosiglitazone did not affect the expression of PPARγ or ABCA1 (Fig. 4A and B). In comparison, expression of alveolar macrophage ABCG1, a target gene of PPARγ, was significantly increased in MWCNT-instilled mice receiving rosiglitazone compared to those receiving normal chow (Fig. 4C). CD36 expression is slightly increased in MWCNT-instilled animals, but was further up-regulated in animals receiving rosiglitazone (Fig. 4D). To assess the rate of alveolar macrophage lipid catabolism we evaluated intracellular and extracellular lipids. Intracellular lipid accumulation was evaluated by determining mean alveolar macrophage diameter. Mice instilled with MWCNT had significantly larger alveolar macrophages compared to controls, while administration of rosiglitazone attenuated the increase in cell size (Fig. 4E). Total cholesterol accumulation in BAL fluid following MWCNT instillation was also reduced by administration of rosiglitazone (Fig. 4F).

4. Discussion

We have described a murine model of MWCNT-induced granulomatous lung disease which closely mimics pulmonary sarcoidosis, including the deficiency of alveolar macrophage PPARγ. The ablation of alveolar macrophage PPARγ exacerbates MWCNT-induced pulmonary granulomatous disease as well as pro-inflammatory alveolar macrophage activation [13]. Here we demonstrate that the PPARγ agonist rosiglitazone significantly limits alveolar macrophage activation, pulmonary granuloma formation and pulmonary lipid dysregulation following MWCNT instillation. These observations suggest that regulation of alveolar macrophage PPARγ may serve as a novel target for limiting pulmonary granulomatous inflammation.

Pretreatment with rosiglitazone limited the expression of pro-inflammatory mediators following MWCNT instillation. PPARγ can regulate inflammatory gene expression by trans-repression, the ability to interfere with the activity of other transcription factors such as NF-κB [16,17]. Alveolar macrophages of pulmonary sarcoidosis patients have significantly higher NF-κB activation compared to healthy individuals [19]. Our studies demonstrate that rosiglitazone inhibits NF-κB nuclear localization in MWCNT-instilled animals. This observation is consistent with an inverse relationship between PPARγ and NF-κB activity. Additionally, CCL2 and osteopontin expression are regulated by NF-κB activity [37,38]. Interestingly, CCL2 or osteopontin-deficient mice develop less severe pulmonary granulomas in response to infectious stimuli [39,40]. These data suggest that such mediators

may play a role in granuloma progression. The upregulation of these mediators in both human sarcoidosis and in MWCNT-instilled mice, beginning as early as ten days post instillation, also supports a critical role for these mediators in pulmonary granulomatous disease progression.

The frequency and severity of granulomatous lesions are attenuated by rosiglitazone 20 days post MWCNT instillation. The reduction of BAL fluid protein concentration in rosiglitazone treated animals also suggests attenuation of total lung injury. Previous reports have noted BAL fluid albumin concentration increased in a dose dependent manner following MWCNT instillation [41]. In addition to the decrease in frequency and severity of granulomas 20 days post-instillation, a decrease in pulmonary carbon content was also observed. Inhaled particulate matter has been shown to clear through pulmonary lymphatics [42,43]. The increase in mediastinal lymph node volume may suggest that carbon is cleared through this pathway when not incorporated into granuloma. Changes in mediastinal lymphadenopathy warrant further study with regard to carbon content and identity of lymph node cells.

In this report, we show the treatment with rosiglitazone significantly limits MWCNT-induced pulmonary lipid accumulation. Our previous studies have shown alveolar macrophages of 60 day MWCNT-instilled animals have increased intracellular lipid accumulation, a phenotype which promotes pro-inflammatory signaling in ABC-lipid transporter deficient macrophages [29,30]. Our data suggest that rosiglitazone increases alveolar macrophage lipid catabolism by promoting uptake and export, by the PPARγ target genes CD36 and ABCG1. The slight increase of CD36 expression observed in alveolar macrophages of MWCNT-instilled animals may be attributed to increased intracellular lipid content. Oxidized lipids have been shown to promote CD36 expression in a PPARγ-independent mechanism [44]. These observations suggest that pulmonary lipid dysregulation following exposure to MWCNT may contribute to alveolar macrophage pro-inflammatory activation.

The current findings support and confirm our previous study examining the role of PPARg deficiency in granulomatous disease [13]. Whereas PPARγ deficiency exacerbates granulomatous disease, ligand-dependent induction of PPARγ activity exerts a protective effect and constrains granuloma size. These data also strongly suggest that the PPARγ pathway responsible for the protective effect is the regulation via target gene activity, of intracellular pro-inflammatory lipid accumulation.

Acknowledgements

ABBREVIATIONS:

ABCA1	ATP-binding cassette lipid transporter-Al
ABCG1	ATP-binding cassette lipid transporter-Gl
BAL	Bronchoalveolar lavage

CD36	Cluster of differentiation-36
NF-κB	Nuclear Factor-Kappa-B
PPARγ	Peroxisome proliferator activated receptor-gamma

References

[1]. Baughman RP, Teirstein AS, Judson MA, Rossman MD, Yeager H, Bresnitz EA, DePalo L, Hunninghake G, Iannuzzi MC, Johns CJ, McLennan G, Moller DR, Newman LS, Rabin DL, Rose C, Rybicki B, Weinberger SE, Terrin ML, Knatterud GL, Cherniak R, Clinical characteristics of patients in a case control study of sarcoidosis, Am. J. Respir. Crit. Care Med. 164 (2001) 1885–1889. [PubMed: 11734441]

[2]. Chen ES, Moller DR, Etiology of sarcoidosis, Clin. Chest Med. 29 (2008) 365–377 vii. [PubMed: 18539232]

[3]. Kajdasz DK, Lackland DT, Mohr LC, Judson MA, A current assessment of rurally linked exposures as potential risk factors for sarcoidosis, Ann. Epidemiol. 11 (2001) 111–117. [PubMed: 11164127]

[4]. Kreider ME, Christie JD, Thompson B, Newman L, Rose C, Barnard J, Bresnitz E, Judson MA, Lackland DT, Rossman MD, Relationship of environmental exposures to the clinical phenotype of sarcoidosis, Chest 128 (2005) 207–215. [PubMed: 16002937]

[5]. Prezant DJ, Dhala A, Goldstein A, Janus D, Ortiz F, Aldrich TK, Kelly KJ, The incidence, prevalence, and severity of sarcoidosis in New York City firefighters, Chest 116 (1999) 1183–1193. [PubMed: 10559074]

[6]. Izbicki G, Chavko R, Banauch GI, Weiden MD, Berger KI, Aldrich TK, Hall C, Kelly KJ, Prezant DJ, World trade center "Sarcoid-Like" granulomatous pulmonary disease in New York city fire department rescue workers, Chest 131 (2007) 1414–1423. [PubMed: 17400664]

[7]. Lam CW, James JT, McCluskey R, Hunter RL, Pulmonary toxicity of singlewall carbon nanotubes in mice 7 and 90 days after intratracheal instillation, Toxicol. Sci. 77 (2004) 126–134. [PubMed: 14514958]

[8]. Muller J, Huaux F, Moreau N, Misson P, Heilier JF, Delos M, Arras M, Fonseca A, Nagy JB, Lison D, Respiratory toxicity of multi-wall carbon nanotubes, Toxicol. Appl. Pharmacol. 207 (2005) 221–231. [PubMed: 16129115]

[9]. Huizar I, Malur A, Midgette YA, Kukoly C, Chen P, Ke PC, Podila R, Rao AM, Wingard CJ, Dobbs L, Barna BP, Kavuru MS, Thomassen MJ, Novel murine model of chronic granulomatous lung inflammation elicited by carbon nanotubes, Am. J. Respir. Cell Mol. Biol. 45 (2011) 858–866. [PubMed: 21398620]

[10]. Iio K, Iio TU, Okui Y, Ichikawa H, Tanimoto Y, Miyahara N, Kanehiro A, Tanimoto M, Nakata Y, Kataoka M, Experimental pulmonary granuloma mimicking sarcoidosis induced by Propionibacterium acnes in mice, Acta Med. Okayama 64 (2010) 75–83. [PubMed: 20424662]

[11]. Chensue SW, Otterness IG, Higashi GI, Forsch CS, Kunkel SL, Monokine production by hypersensitivity (Schistosoma mansoni egg) and foreign body (Sephadex bead)-type granuloma macrophages. Evidence for sequential production of IL-1 and tumor necrosis factor, J. Immunol. 142 (1989) 1281–1286. [PubMed: 2464642]

[12]. Kunkel S, Lukacs NW, Strieter RM, Chensue SW, Animal models of granulomatous inflammation, Semin. Respir. Infect. 13 (1998) 221–228. [PubMed: 9764953]

[13]. Huizar I, Malur A, Patel J, McPeek M, Dobbs L, Wingard C, Barna BP, Thomassen MJ, The role of PPARgamma in carbon nanotube-elicited granulomatous lung inflammation, Respir. Res. 14 (2013) 7. [PubMed: 23343389]

[14]. Mohan A, Malur A, McPeek M, Barna BP, Schnapp LM, Thomassen MJ, Gharib SA, Transcriptional survey of alveolar macrophages in a murine model of chronic granulomatous inflammation reveals common themes with human sarcoidosis, Am. J. Physiol. Lung Cell Mol. Physiol. 314 (2018) L617–625. [PubMed: 29212802]

[15]. Ricote M, Welch JS, Glass CK, Regulation of macrophage gene expression by the peroxisome proliferator-activated receptor-gamma, Horm. Res. 54 (2000) 275–280. [PubMed: 11595817]

[16]. Ghisletti S, Huang W, Ogawa S, Pascual G, Lin ME, Willson TM, Rosenfeld MG, Glass CK, Parallel SUMOylation-dependent pathways mediate gene-and signal-specific transrepression by LXRs and PPARgamma, Mol. Cell 25 (2007) 57–70. [PubMed: 17218271]

[17]. Ricote M, Glass CK, PPARs and molecular mechanisms of transrepression, Biochim. Biophys. Acta 1771 (2007) 926–935. [PubMed: 17433773]

[18]. Bonfield TL, Farver CF, Barna BP, Malur A, Abraham S, Raychaudhuri B, Kavuru MS, Thomassen MJ, Peroxisome proliferator-activated receptor-gamma is deficient in alveolar macrophages from patients with alveolar proteinosis, Am. J. Respir. Cell Mol. Biol. 29 (2003) 677–682. [PubMed: 12805087]

[19]. Culver DA, Barna BP, Raychaudhuri B, Bonfield TL, Abraham S, Malur A, Farver CF, Kavuru MS, Thomassen MJ, Peroxisome proliferator-activated receptor gamma activity is deficient in alveolar macrophages in pulmonary sarcoidosis, Am. J. Respir. Cell Mol. Biol. 30 (2004) 1–5. [PubMed: 14512375]

[20]. Kobayashi M, Thomassen MJ, Rambasek T, Bonfield TL, Raychaudhuri B, Malur A, Winkler AR, Barna BP, Goldman SJ, Kavuru MS, An inverse relationship between peroxisome proliferator-activated receptor gamma and allergic airway inflammation in an allergen challenge model, Ann. Allergy Asthma Immunol. 95 (2005) 468–473. [PubMed: 16312170]

[21]. Malur A, Mccoy AJ, Arce S, Barna BP, Kavuru MS, Malur AG, Thomassen MJ, Deletion of PPARγ in alveolar macrophages is associated with a Th-1 pulmonary inflammatory response, J. Immunol. 182 (2009) 5816–5822. [PubMed: 19380830]

[22]. Baker AD, Malur A, Barna BP, Ghosh S, Kavuru MS, Malur AG, Thomassen MJ, Targeted PPAR{gamma} deficiency in alveolar macrophages disrupts surfactant catabolism, J. Lipid Res. 51 (2010) 1325–1331. [PubMed: 20064973]

[23]. Baker AD, Malur A, Barna BP, Kavuru MS, Malur AG, Thomassen MJ, PPARgamma regulates the expression of cholesterol metabolism genes in alveolar macrophages, Biochem. Biophys. Res. Commun. 393 (2010) 682–687. [PubMed: 20170635]

[24]. Pennings M, Meurs I, Ye D, Out R, Hoekstra M, Van Berkel TJ, Van EM, Regulation of cholesterol homeostasis in macrophages and consequences for atherosclerotic lesion development, FEBS Lett. 580 (2006) 5588–5596. [PubMed: 16935283]

[25]. Bates SR, Tao JQ, Collins HL, Francone OL, Rothblat GH, Pulmonary abnormalities due to ABCA1 deficiency in mice, Am. J. Physiol. Lung Cell Mol. Physiol. 289 (2005) L980–L989. [PubMed: 16055479]

[26]. Koseki M, Hirano K, Masuda D, Ikegami C, Tanaka M, Ota A, Sandoval JC, Nakagawa-Toyama Y, Sato SB, Kobayashi T, Shimada Y, Ohno-Iwashita Y, Matsuura F, Shimomura I, Yamashita S, Increased lipid rafts and accelerated lipopolysaccharide-induced tumor necrosis factor-alpha secretion in Abca1-deficient macrophages, J. Lipid Res. 48 (2007) 299–306. [PubMed: 17079792]

[27]. Wojcik AJ, Skaflen MD, Srinivasan S, Hedrick CC, A critical role for ABCG1 in macrophage inflammation and lung homeostasis, J. Immunol. 180 (2008) 4273–4282. [PubMed: 18322240]

[28]. Baldan A, Gomes AV, Ping P, Edwards PA, Loss of ABCG1 results in chronic pulmonary inflammation, J. Immunol. 180 (2008) 3560–3568. [PubMed: 18292583]

[29]. Yvan-Charvet L, Welch C, Pagler TA, Ranalletta M, Lamkanfi M, Han S, Ishibashi M, Li R, Wang N, Tall AR, Increased inflammatory gene expression in ABC transporter-deficient macrophages: free cholesterol accumulation, increased signaling via toll-like receptors, and neutrophil infiltration of atherosclerotic lesions, Circulation 118 (2008) 1837–1847. [PubMed: 18852364]

[30]. Barna BP, McPeek M, Malur A, Fessler MB, Wingard CJ, Dobbs L, Verbanac KM, Bowling M, Judson MA, Thomassen MJ, Elevated MicroRNA-33 in sarcoidosis and a carbon nanotube model of chronic granulomatous disease, Am. J. Respir. Cell Mol. Biol. 54 (2016) 865–871. [PubMed: 26641802]

[31]. Livak KJ, Schmittgen TD, Analysis of relative gene expression data using real-time quantitative PCR and the 2(-Delta Delta C(T)) Method, Methods 25 (2001)402–408. [PubMed: 11846609]

[32]. Song G, Darr DB, Santos CM, Ross M, Valdivia A, Jordan JL, Midkiff BR, Cohen S, Nikolaishvili-Feinberg N, Miller CR, Tarrant TK, Rogers AB, Dudley AC, Perou CM, Zamboni WC, Effects of tumor microenvironment heterogeneity on nanoparticle disposition and efficacy in breast cancer tumor models, Clin. Canc. Res. 20 (2014) 6083–6095.

[33]. Van den Broeck W, Derore A, Simoens P, Anatomy and nomenclature of murine lymph nodes: descriptive study and nomenclatory standardization in BALB/cAnNCrl mice, J.Immunol. Methods 312 (2006) 12–19. [PubMed: 16624319]

[34]. O'Regan AW, Chupp GL, Lowry JA, Goetschkes M, Mulligan N, Berman JS, Osteopontin is associated with T cells in sacroid granulomas and has T cell adhesive and cytokin-like properties in vitro, J. Immunol. 162 (1999) 1024–1031. [PubMed: 9916729]

[35]. Palchevskiy V, Hashemi N, Weigt SS, Xue YY, Derhovanessian A, Keane MP, Strieter RM, Fishbein MC, Deng JC, Lynch III JP, Elashoff R, Belperio JA, Immune response CC chemokines CCL2 and CCL5 are associated with pulmonary sarcoidosis, Fibrogenesis Tissue Repair 4 (2011) 10. [PubMed: 21463523]

[36]. Barna BP, Huizar I, Malur A, McPeek M, Marshall I, Jacob M, Dobbs L, Kavuru MS, Thomassen MJ, Carbon nanotube-induced pulmonary granulomatous disease: twist1 and alveolar macrophage m1 activation, Int. J. Mol. Sci. 14 (2013) 23858–23871. [PubMed: 24322444]

[37]. Martin T, Cardarelli PM, Parry GC, Felts KA, Cobb RR, Cytokine induction of monocyte chemoattractant protein-1 gene expression in human endothelial cells depends on the cooperative action of NF-kappa B and AP-1, Eur. J. Immunol. 27 (1997) 1091–1097. [PubMed: 9174597]

[38]. Zhao W, Wang L, Zhang M, Wang P, Zhang L, Yuan C, Qi J, Qiao Y, Kuo PC, Gao C, NF-kappaB-and AP-1-mediated DNA looping regulates osteopontin transcription in endotoxin-stimulated murine macrophages, J. Immunol. 186 (2011) 3173–3179. [PubMed: 21257959]

[39]. Lu B, Rutledge BJ, Gu L, Fiorillo J, Lukacs NW, Kunkel SL, North R, Gerard C, Rollins BJ, Abnormalities in monocyte recruitment and cytokine expression in monocyte chemoattractant protein 1-deficient mice, J. Exp. Med. 187 (1998) 601–608. [PubMed: 9463410]

[40]. O'Regan AW, Hayden JM, Body S, Liaw L, Mulligan N, Goetschkes M, Berman JS, Abnormal pulmonary granuloma formation in osteopontin-deficient mice, Am. J. Respir. Crit. Care Med. 164 (2001) 2243–2247. [PubMed: 11751194]

[41]. Porter DW, Hubbs AF, Mercer RR, Wu N, Wolfarth MG, Sriram K, Leonard S, Battelli L, Schwegler-Berry D, Friend S, Andrew M, Chen BT, Tsuruoka S, Endo M, Castranova V, Mouse pulmonary dose-and time courseresponses induced by exposure to multi-walled carbon nanotubes, Toxicology 269 (2010) 136–147. [PubMed: 19857541]

[42]. Snipes MB, Long-term retention and clearance of particles inhaled by mammalian species, Crit. Rev. Toxicol. 20 (1989) 175–211. [PubMed: 2692607]

[43]. Aiso S, Kubota H, Umeda Y, Kasai T, Takaya M, Yamazaki K, Nagano K, Sakai T, Koda S, Fukushima S, Translocation of intratracheally instilled multiwall carbon nanotubes to lung-associated lymph nodes in rats, Ind. Health 49 (2011) 215–220. [PubMed: 21173528]

[44]. D'Archivio M, Scazzocchio B, Filesi C, Vari R, Maggiorella MT, Sernicola L, Santangelo C, Giovannini C, Masella R, Oxidised LDL up-regulate CD36 expression by the Nrf2 pathway in 3T3-L1 preadipocytes, FEBS Lett. 582 (2008) 2291–2298. [PubMed: 18514070]
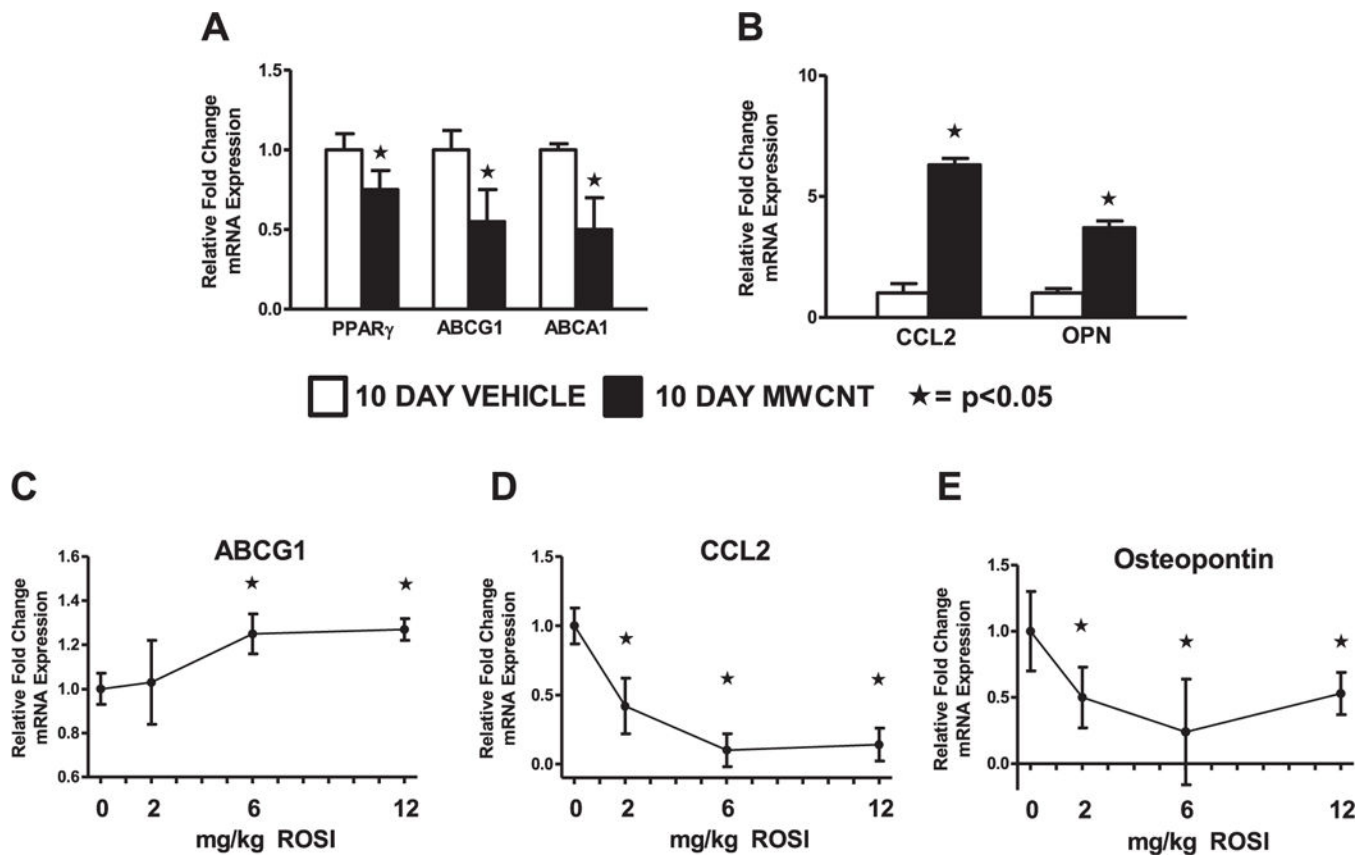
Fig. 1. Rosiglitazone Regulates Alveolar Macrophage Gene Expression 10 days following MWCNT instillation.

Quantitative-PCR analysis of the lipid regulatory genes (A) peroxisome proliferator activated receptor-γ (PPARγ), ATP-binding cassette lipid transporter-G1 (ABCG1), and ABCA1; and inflammatory mediators (B) CCL2 and osteopontin (OPN) in BAL cells of vehicle or MWCNT-instilled mice. Effect of rosiglitazone dose curve on alveolar macrophage (C) ABCG1, (D) CCL2 and (E) osteopontin expression. ★$p < 0.05$, n   3/ treatment.
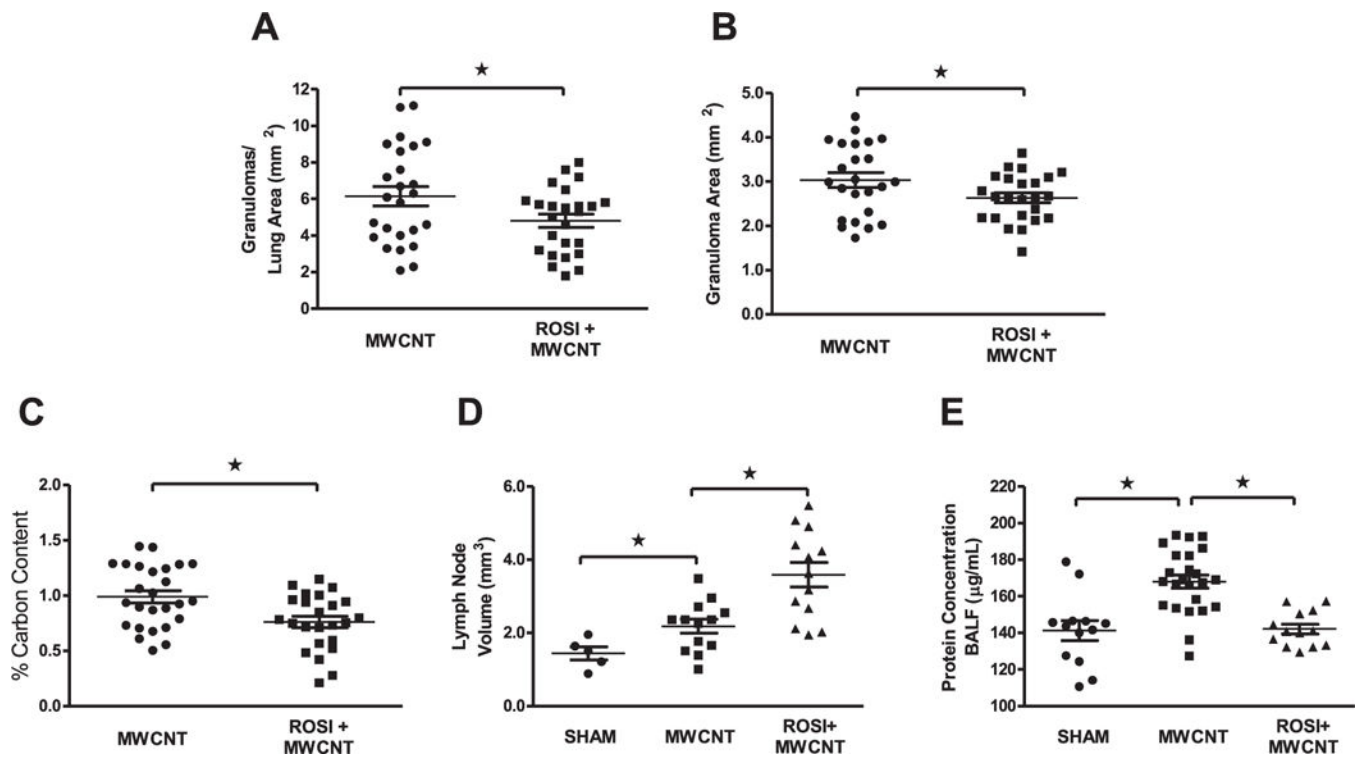
Fig. 2. Rosiglitazone Inhibits Pulmonary Granuloma Formation 20 days post MWCNT Instillation.

Quantitative analysis of H&E stained lung tissue was utilized to evaluate (A) the average number of granulomas, (B) average granuloma size, (C) and total carbon deposition in MWCNT-instilled animals receiving normal chow or rosiglitazone (6 mg/kg). Evaluation of (D) mediastinal lymph node volume and (E) BAL-fluid protein concentration in vehicle and MWCNT-instilled animals receiving normal chow or rosiglitazone (6 mg/ kg). ★$p < 0.05$, n 5/treatment.
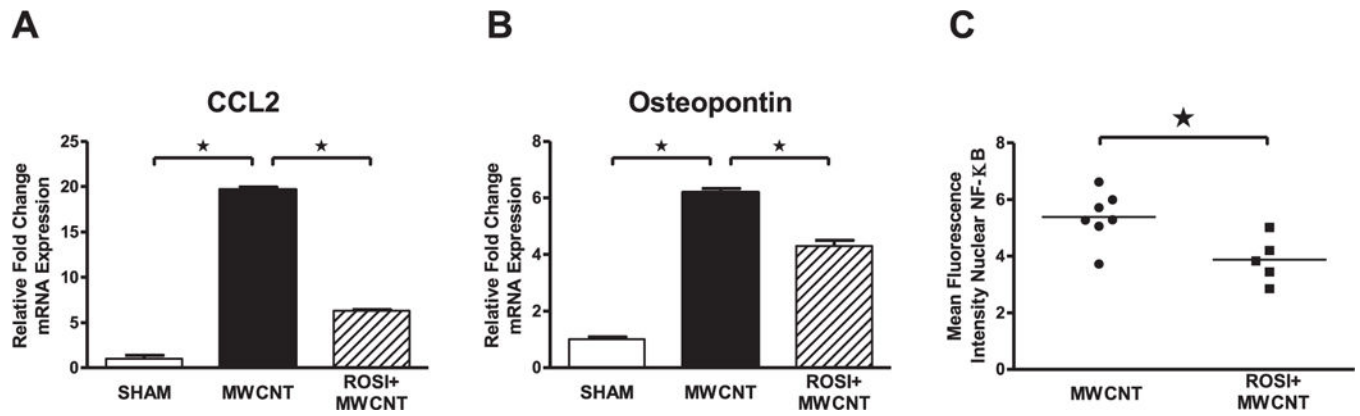
Fig. 3. Rosiglitazone Reduces Alveolar Macrophage Activation 20 days post MWCNT-Instillation.
Quantitative-PCR analysis of (A) CCL2 and (B) osteopontin expression in BAL cells of vehicle or MWCNT-instilled animals receiving normal chow or rosiglitazone (6 mg/kg). (C) Mean fluorescence intensity of nuclear NF-κB p65 protein in MWCNT-instilled animals receiving normal chow or rosiglitazone (6 mg/kg), 99 cells/animal. ★p < 0.01, n 5/treatment.
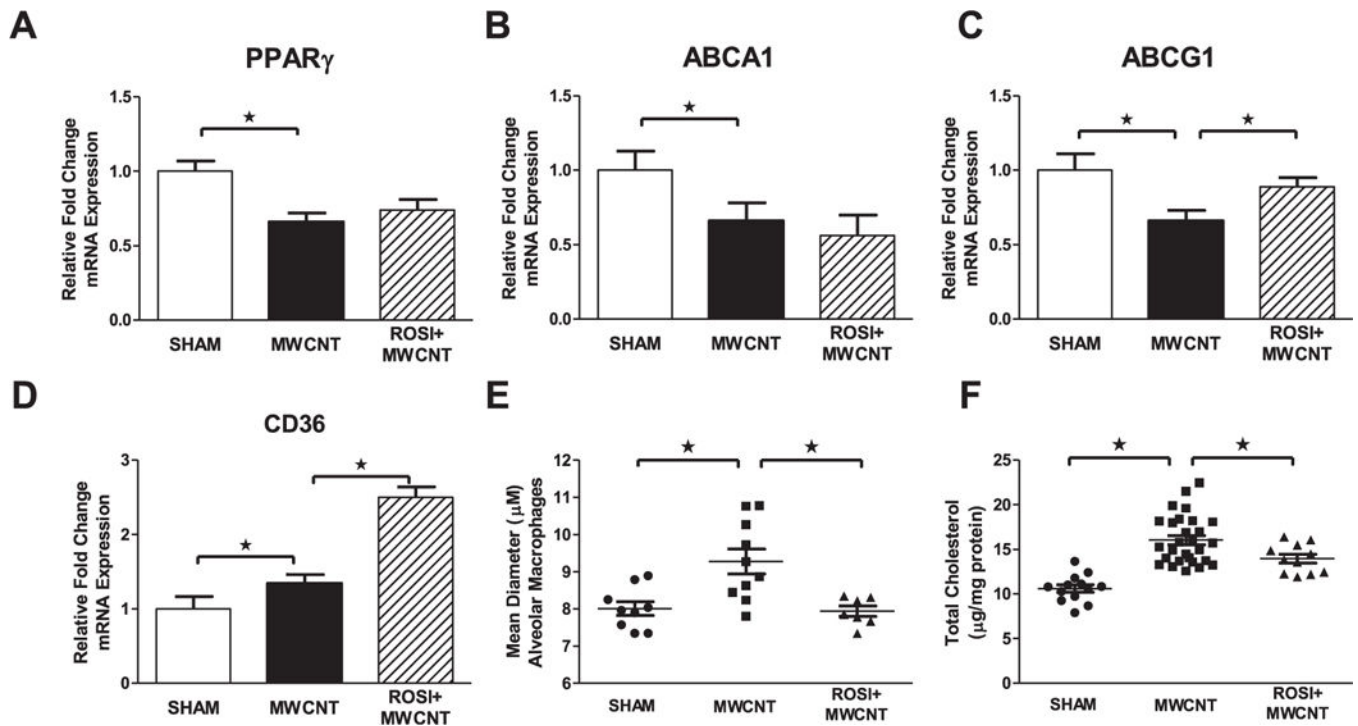
Fig. 4. Rosiglitazone limits pulmonary dyslipidemia 20 days following MWCNT-instillation.
Quantitative-PCR analysis of the lipid regulatory genes (A) PPARγ (B) ABCA1, (C) ABCG1 and (D) CD36 in vehicle or MWCNT-instilled animals receiving normal chow or rosiglitazone (6 mg/kg). Evaluation of (E) mean alveolar macrophage diameter and (E) total cholesterol content of BAL fluid of vehicle and MWCNT-instilled mice receiving normal chow or rosiglitazone (6 mg/kg). $\star p < 0.01$, n 5/treatment.